Proceedings of the 7th GACM Colloquium on Computational Mechanics for Young Scientists from Academia and Industry October 11-13, 2017 in Stuttgart, Germany

Regularisation of gradient-enhanced damage coupled to finite plasticity

Leon Sprave[1]* and Andreas Menzel[1,2]

Micro Abstract
An isotropic gradient-enhanced damage formulation is coupled to finite von Mises plasticity. In the context of finite elements an additional field variable, representing nonlocal damage, is introduced. In a multisurface approach, the evolution of damage and plasticity are governed by their respective criteria. Simulation results are compared to experimental data to verify the model.

[1]Institute of Mechanics, TU Dortmund University, Dortmund, Germany
[2]Division of Solid Mechanics, Lund University, P.O. Box 118, SE-221 00 Lund, Sweden
***Corresponding author**: leon.sprave@tu-dortmund.de

Introduction

After giving a short summary of the gradient-enhanced isotropic damage model coupled to finite plasticity, an alternative element formulation — the F-bar formulation from [1] — is discussed to overcome problems related to volumetric locking. The result section compares the standard and F-bar formulations and shows the regularisation of the framework.

1 Gradient-enhanced isotropic damage coupled to finite plasticity

The gradient-enhancement follows the approach of [2, 7]. The theory presented here is an extension to large strain of the formulation established in [3]. Large strain damage models in this regularisation framework are also proposed in [4, 8].
An additional field variable ϕ is introduced and connected to the local damage variable d by means of a penalty term in the free Helmholtz energy Ψ. Consequently, ϕ is called nonlocal damage field in the following. Now, penalising the gradient of the nonlocal damage field indirectly also penalises the gradient of the local damage variable without the necessity to compute the gradient of d directly. Thereby, the implementation of the gradient-enhancement becomes independent of the formulation of the local material model incorporating the local damage variable d.
The free Helmholtz energy is completed by an elastic part formulated with the help of the elastic logarithmic strain tensor $\boldsymbol{\varepsilon}^{\mathrm{e}}$, see e.g. [5], and a plastic contribution taking linear hardening into account, i.e.

$$\Psi(\boldsymbol{\varepsilon}^{\mathrm{e}}, \phi, d, \alpha) = \frac{K}{2}\, f^{\mathrm{vol}}(d)\,[\mathrm{tr}(\boldsymbol{\varepsilon}^{\mathrm{e}})]^2 + \mu\, f^{\mathrm{iso}}(d)\, \boldsymbol{\varepsilon}^{\mathrm{e}} : \boldsymbol{\varepsilon}^{\mathrm{e}} + \frac{h}{2}\,\alpha^2 + \frac{c_{\mathrm{d}}}{2}\,\|\nabla_{\boldsymbol{X}}\phi\|^2 + \frac{\beta_{\mathrm{d}}}{2}\,[\phi - d]^2 \,. \quad (1)$$

The volumetric and isochoric elastic energy contributions are weighted differently with damage functions $f^\bullet(d)$ defined as

$$f^\bullet : \mathbb{R}_0^+ \to]0,1] \quad \text{with} \quad f^\bullet(d) := \exp(-\eta_\bullet\, d)\,, \quad (2)$$

such that the local damage variable d is unbounded towards infinity. Following standard thermodynamics, the driving forces, the Mandel stress $\boldsymbol{m}^{\mathrm{t}}$ and the damage driving force q, are defined as

$$\boldsymbol{m}^{\mathrm{t}} := 2\,\frac{\partial \Psi}{\partial \boldsymbol{b}^{\mathrm{e}}} \cdot \boldsymbol{b}^{\mathrm{e}}\,, \qquad \boldsymbol{m}^{\mathrm{t}}_{\mathrm{eff}} := \boldsymbol{m}^{\mathrm{t}}\; [f^m(d)]^{-1} \qquad \text{and} \qquad q := -\frac{\partial \Psi}{\partial d}\,. \quad (3)$$

The postulate of equivalent strain is employed, defining the effective Mandel stress $\boldsymbol{m}^{\mathrm{t}}_{\mathrm{eff}}$, in order to enable evolution of plasticity even after the initiation of damage evolution. By using a multisurface approach, the evolution of damage and plasticity is governed by their respective criteria — the damage criterion Φ^{d} and a von Mises yield criterion including linear hardening Φ^{p}

$$\Phi^{\mathrm{d}}(q,d) = q - q_{\min}\left[1 - f^{q}(d)\right]^{n} \qquad \text{and} \qquad \Phi^{\mathrm{p}}(\boldsymbol{m}^{\mathrm{t}},\beta,d) = \|\operatorname{dev}(\boldsymbol{m}^{\mathrm{t}}_{\mathrm{eff}})\| - \sqrt{\frac{2}{3}}\left[\sigma^{0}_{\mathrm{y}} - \beta\right]\,. \quad (4)$$

The associative evolution equations are discretised in time with the help of the exponential map in the case of the plastic part and a standard backward Euler scheme for the damage part. Hence, it is only necessary to solve for the two Lagrange multipliers connected to the yield and damage criterion respectively at every quadrature point. The double set of Karush-Kuhn-Tucker conditions is solved here with an active-set scheme.

2 F-bar formulation

The standard finite element formulation of the previously summarised material model exhibits reduced regularisation behaviour [6]. A possible reason might be the isochoric evolution of plasticity which can result in volumetric locking if low order elements are used. Instead of using higher order elements, which are numerically expensive, the F-bar formulation from [1] is a numerically inexpensive alternative. The deformation gradient at each quadrature point $\boldsymbol{F}$ is split into its volumetric and isochoric part. The volumetric part is replaced by the volumetric part of the deformation gradient evaluated in the center of the current element $\boldsymbol{F}_0$, which defines a new deformation gradient

$$\bar{\boldsymbol{F}} = \left[\frac{\det(\boldsymbol{F}_0)}{\det(\boldsymbol{F})}\right]^{\frac{1}{3}} \boldsymbol{F}\,. \qquad (5)$$

These modifications only lead to implementation changes in the element formulation, since the material response is computed for $\bar{\boldsymbol{F}}$. The tangents computed at material point level are derivatives with respect to $\bar{\boldsymbol{F}}$, which can be transformed to derivatives with respect to $\boldsymbol{F}$ on element level. Considering an element formulation based on the Piola stress tensor $\boldsymbol{P}$, the derivative with respect to the displacements $\boldsymbol{u}^{eA}$of element e and node A reads

$$\frac{\mathrm{d}\boldsymbol{P}}{\mathrm{d}\boldsymbol{u}^{eA}} = \frac{\mathrm{d}\boldsymbol{P}}{\mathrm{d}\bar{\boldsymbol{F}}} : \left[\frac{\partial\bar{\boldsymbol{F}}}{\partial\boldsymbol{F}} : \frac{\mathrm{d}\boldsymbol{F}}{\mathrm{d}\boldsymbol{u}^{eA}} + \frac{\partial\bar{\boldsymbol{F}}}{\partial\boldsymbol{F}_0} : \frac{\mathrm{d}\boldsymbol{F}_0}{\mathrm{d}\boldsymbol{u}^{eA}}\right]\,. \qquad (6)$$

3 Simulation results

All simulations are carried out using a notched plate — symmetry is used to reduce the problem size — discretised with 1350, 5400 or 12150 number of elements. The notch is a circular hole with a radius of a quarter of the width of the plate. The elastic and plastic material parameters are taken from measurements on DP800, while the damage related parameters are chosen to qualitatively match the observed experimental behaviour. The parameters listed in Table 1 represent the reference set, such that only parameters deviating from this set are mentioned in the following.

E	ν	σ^0_y	h	$q_{\min}$	n	η_{vol}	η_{iso}	η_q	η_m	c_{d}	β_{d}
GPa	–	MPa	GPa	MPa	–	–	–	–	–	N	MPa
208	0.3	809	6	2.0	2/3	0.7	0.7	10	0.7	500	500

Table 1. List of material parameters used in the reference set.

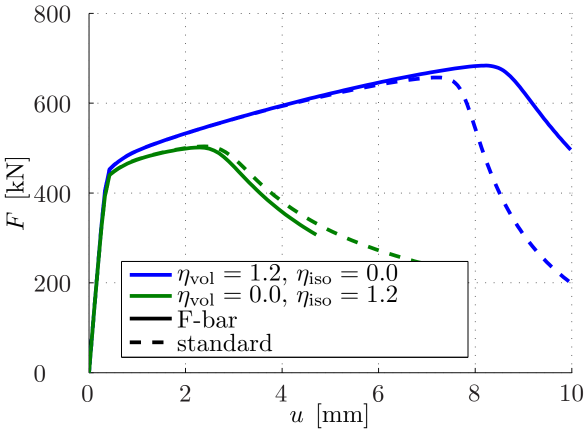

Figure 1. Load displacement diagram of the notched plate under tension comparing the F-bar formulation (continuous line) with the standard element (dashed line) for two parameter sets
(blue: $\eta_{\mathrm{iso}} = 0.0$, $q_{\mathrm{min}} = 1.75\,\mathrm{MPa}$;
green: $\eta_{\mathrm{vol}} = 0.0$, $q_{\mathrm{min}} = 3.0\,\mathrm{MPa}$).

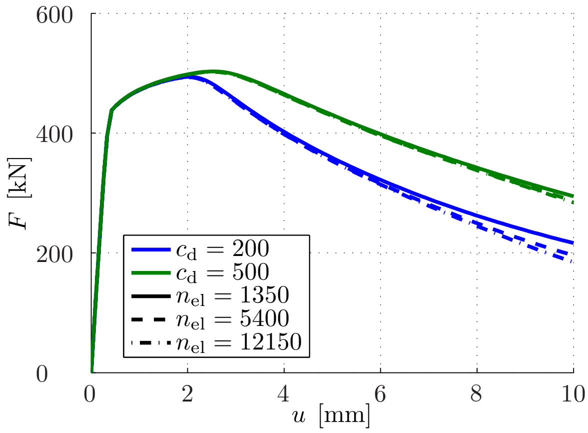

Figure 2. Load displacement diagram of the notched plate comparing the response for a regularisation parameter $c_{\mathrm{d}} = 200\,\mathrm{N}$ with $c_{\mathrm{d}} = 500\,\mathrm{N}$ for discretisations with 1350, 5400, and 12150 elements.

3.1 Comparison of standard and F-bar formulation

Figure 1 compares the standard and F-bar formulation by separating the influences from volumetric and isochoric strains on the evolution of damage. All responses display distinct elastic, plastic and damage dominated regions. For damage driven by volumetric deformations (blue curve) the standard formulation leads to earlier initiation of damage. Even though the standard formulation is usually stiffer than e.g. an F-bar formulation, in the context of damage this has to be interpreted differently. The stiffer response has its origin in an overestimation of the volumetric strains which leads here to a higher damage driving force and consequently to earlier violation of the damage criterion.
If the volumetric strain does not influence the evolution of damage ($\eta_{\mathrm{vol}} = 0.0$, green curve) the intuitive result of a stiffer response of the standard formulation is observed.

3.2 Regularisation

Previously, for the standard formulation, a sufficient regularisation could not be observed [6]. Implementing the F-bar formulation now shows satisfying regularisation, see Figures 2 and 3. In Figure 2 the load displacement diagrams for three different discretisations (depicted by different line styles) and two values of the gradient parameter c_{d} are compared. Again, it is possible to identify an elastic, a plasic and damage dominated region. Clearly, for $c_{\mathrm{d}} = 500\,\mathrm{N}$ (green curves) the responses of different discretisations coincide, exemplifying a sufficient regularisation. Also for $c_{\mathrm{d}} = 200\,\mathrm{N}$ (blue curves) the responses only slightly deviate after damage evolved for some time. These small deviations can stem from even smaller numerical pertubations earlier in the computation, which in the damage region leads to a slightly different path taken.
Proper regularisation for the case of $c_{\mathrm{d}} = 200\,\mathrm{N}$ can also be seen in Figure 3. One observes a zone of damage with defined width at the smallest cross-section. For both discretisations the width of the damage zone is equal, which is clearly exhibited in the undeformed plot (b).

Conclusions

The damage formulation was enhanced by the gradient of an additionally introduced nonlocal field to circumvent direct calculation of the gradient of the local damage variable. A damage model coupled to finite plasticity with separate damage and yield criterion was implemented. The F-bar formulation, to prevent volumetric locking, was compared to the standard formulation

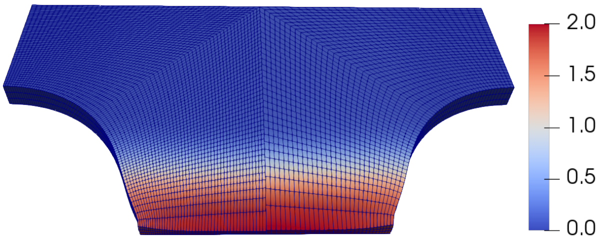

a) deformed contour plot of d

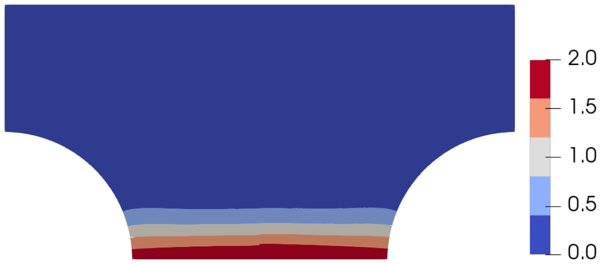

b) undeformed contour plot of d

Figure 3. Notched plate under tension with reference parameter set and $c_{\mathrm{d}} = 200\,\mathrm{N}$. Contour plots of the damage variable extrapolated to the nodes. The left half of each image shows a discretisation with 12150 elements and on the right half (mirrored) a discretisation with 5400 elements is depicted. The left image (a) shows deformed meshes while the right image (b) shows the undeformed state.

for damage models. Within the standard formulation damage initiates earlier compared to the F-bar formulation. While the standard element formulation seemed to not perfectly regularise, the F-bar formulation analysed here exhibited excellent regularisation properties.

Acknowledgements

The financial support of the German Research Foundation (DFG), Transregio 188 "Damage Controlled Forming Processes" (TRR 188) within project C2, is gratefully acknowledged.

References

[1] E. de Souza Neto, D. Perić, M. Dutko, and D. Owen. Design of simple low order finite elements for large strain analysis of nearly incompressible solids. *International Journal of Solids and Structures*, 33(20):3277–3296, 1996.

[2] B. J. Dimitrijevic and K. Hackl. A method for gradient enhancement of continuum damage models. *Technische Mechanik*, 28(1):43–52, 2008.

[3] B. Kiefer, T. Waffenschmidt, L. Sprave, and A. Menzel. A gradient-enhanced damage model coupled to plasticity—multi-surface formulation and algorithmic concepts. *International Journal of Damage Mechanics*, 2017. DOI:10.1177/1056789516676306.

[4] C. Polindara, T. Waffenschmidt, and A. Menzel. A computational framework for modelling damage-induced softening in fibre-reinforced materials – application to balloon angioplasty. *International Journal of Solids and Structures*, 2017.

[5] J. C. Simo. Numerical analysis and simulation of plasticity. In P. G. Ciarlet and J. L. Lions, editors, *Numerical Methods for Solids (Part 3) Numerical Methods for Fluids (Part 1)*, volume VI of *Handbook of Numerical Analysis*, pages 183–499. Elsevier Science B.V., 1998.

[6] L. Sprave and A. Menzel. A multisurface model for gradient-enhanced damage coupled to finite plasticity. *Proc. Appl. Math. Mech.*, accepted for publication, 2017.

[7] P. Steinmann and E. Stein. A unifying treatise of variational principles for two types of micropolar continua. *Acta Mechanica*, 121(1-4):215–232, 1997.

[8] T. Waffenschmidt, C. Polindara, A. Menzel, and S. Blanco. A gradient-enhanced large-deformation continuum damage model for fibre-reinforced materials. *Computer Methods in Applied Mechanics and Engineering*, 268:801–842, 2014.